The Matuyama Chronozone at ODP Site 982 (Rockall Bank): Evidence for Decimeter-Scale Magnetization Lock-in Depths

J. E. T. Channell

Department of Geological Sciences, University of Florida, Gainesville, Florida

Y. Guyodo[1]

Institute for Rock Magnetism, Department of Geology and Geophysics, University of Minnesota, Minneapolis, Minnesota

At ODP Site 982, located on the Rockall Bank, component magnetizations define a polarity stratigraphy from the middle part of the Brunhes Chronozone to the top of the Gauss Chronozone (0.3–2.7 Ma). The Cobb Mountain and Reunion subchronozones correlate to marine isotope stages (MIS) 35 and 81, respectively. The Gauss/Matuyama boundary correlates to the base of MIS 103. The slope of the natural remanence (NRM) versus the anhysteretic remanence (ARM) during stepwise alternating field demagnetization is close to linear ($r > 0.9$) for the 900–1700 ka interval indicating similarity of NRM and ARM coercivity spectra. The normalized remanence (NRM/ARM) can be matched to paleointensity records from ODP Sites 983/984 (Iceland Basin) and from sites in the Pacific Ocean. The age model based on $\delta^{18}O$ stratigraphy at ODP Site 982 indicates sedimentation rates in the 1–4 cm/kyr range. At ODP Site 980/981, located ~200 km SE of Site 982 on the eastern flank of the Rockall Plateau, sedimentation rates are 2–7 times greater. According to the $\delta^{18}O$ age models at Site 982 and Site 980/981, the boundaries of the Jaramillo, Cobb Mountain, Olduvai and Reunion subchronozones appear older at Site 982 by 10–15 kyr. We model the lock-in of magnetization using a sigmoidal magnetization lock-in function incorporating a surface mixed layer (base at depth M corresponding to 5% lock-in) and a lock-in depth (L) below M at which 50% lock-in is achieved. The observed age offsets can be simulated by values of DM (difference between values of M at Sites 982 and 980/981) in the 16–23 cm range, and values of L <10 cm. The low values of L imply that the magnetization is rapidly locked (within 10 cm) after sediment passes through the decimeter-scale surface mixed-layer.

1. INTRODUCTION

ODP Site 982 (at 57.52°N, 15.87°W, 1135 m water depth) is located in the Hatton-Rockall Basin, a small depression on the Rockall Plateau (Figure 1). The site has provided a coupled magnetic/$\delta^{18}O$ record for the 0.3–2.7 Ma interval. The record can be used to correlate polarity reversals to marine isotope

[1] Now at Laboratoire des Sciences du Climat et de l'Environnement, Gif-sur-Yvette, France.

Book Title
Book Series

10.1029/Series#LettersChapter#

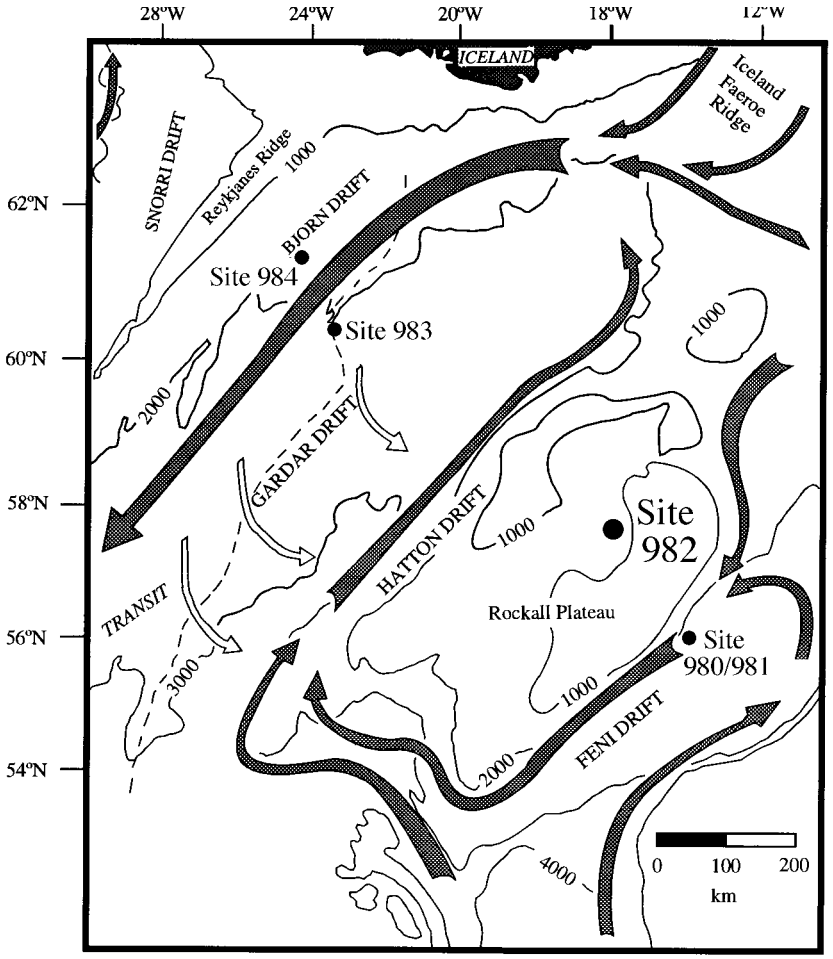

Figure 1. Location map for ODP Site 982. Bathymetry in meters. Dashed line indicates crest of Gardar Drift. Arrows indicate inferred bottom current flows [after *Manley and Caress*, 1994; *McCave et al*., 1980].

stages (MIS), and provides a normalized remanence (paleointensity) record for comparison with other records spanning the same time interval.

The correlation of Plio-Pleistocene isotopic stages to polarity chrons and subchrons has been established using data from DSDP Sites 607/609 [*Raymo et al*., 1989], ODP Site 659 [*Tiedemann et al*., 1994], ODP Site 846/849 [*Shackleton et al.*, 1995a; *Schneider*, 1995], ODP Site 983/984 [*Channell and Kleiven*, 2000; *Channell et al*., 2002] and Italian land sections [*Lourens et al*., 1996]. The correlation is not always straightforward due to uncertainties in interpretation of either the MIS or the magnetic stratigraphy. For example, the boundaries of the Olduvai Subchronozone and the Gauss-Matuyama boundary at ODP Site 659 are poorly defined [*Tauxe et al*., 1989], and the lack of foraminifera in the Matuyama Chronozone at ODP Site 983/984 requires that the susceptibility record be used as a proxy for $\delta^{18}O$ [*Channell et al*., 2002].

An additional motive for this study is that the comparison of polarity chron/MIS correlations for different sedimentation rates offers the possibility of gaining insights into the nature of magnetization lock-in. ODP Site 980/981 located on the eastern slope of the Rockall Plateau (Figure 1) has sedimentation rates 2–7 times greater than at Site 982. High resolution magnetic and isotope records for the Matuyama Chronozone at Site 980/981 have been published elsewhere [*Channell and Raymo*, 2003; *Channell et al*., 2003]. Here we report the magnetic and isotope records from ODP Site 982, and we compare these records with those from Site 980/981.

2. LITHOSTRATIGRAPHY AND AGE MODEL

The sedimentary sequence recovered at ODP Site 982 comprises nannofossil ooze with clay and silt [*Shipboard Scientific Party*, 1996]. The composite section, the optimal section

recovered at the site, was compiled from the shipboard multisensor track (MST) as a splice from the four holes drilled at the site [*Shipboard Scientific Party*, 1996]. This paper deals with the 7–66 meters composite depth (mcd) interval, correlative to the 0.3– 2.7 Ma time interval. The 0–7 mcd interval was not sampled due to drilling disturbance.

Samples for stable isotope analyses were collected at 5 cm intervals from the composite section at Site 982. Stable isotope data were acquired from two benthic foraminifera, *Cibicidoides wuellerstorfi* and *Cibicidoides kullenbergi* (Figure 2). Oxygen isotopic ratios were measured on carbon dioxide gas released on treatment with orthophosphoric acid at 90°C using a VG Isogas mass spectrometer at the University of Florida. Values are reported relative to PDB. The analytical procedure, and the benthic and planktic isotope records for the last 1.2 Myrs from Site 982, have been reported elsewhere [*Venz et al*., 1999; *Flower et al*., 2000; *Kleiven et al*., 2003].

Carbonate percentage, calculated from reflectance data and coulometric titration, varies widely in the 90–20% range [*Ortiz et al*., 1999; *Venz et al*., 1999]. Highs in susceptibility (lows in carbonate) are associated with glacial isotopic stages (Figure 2), reflecting enhanced surface water (carbonate) productivity during interglacial stages. Highs in susceptibility also correspond to highs in percentage ice rafted debris [*Venz et al*., 1999]. Down-section from just above the Gauss-Matuyama boundary, located at 57.3 mcd, the percentage carbonate values are uniformly high and volume susceptibility values are uniformly low (Figure 2).

We construct the age model for Site 982 by matching the benthic $\delta^{18}O$ record to the chronology of Shackleton et al.

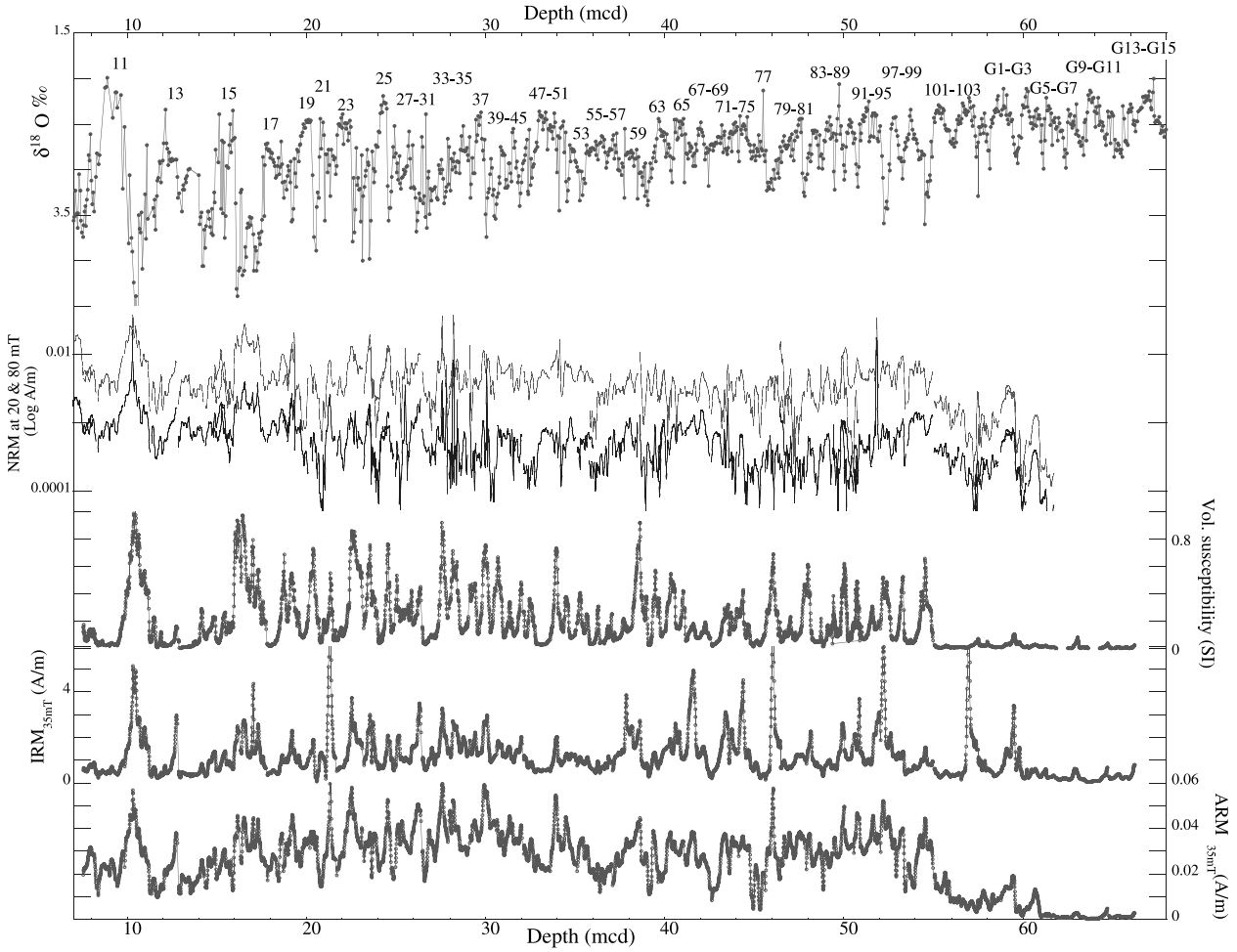

Figure 2. ODP Site 982: benthic $\delta^{18}O$ data [*Venz et al*., 1999; *Flower et al*., 2000; *Kleiven et al*., 2003] with marine isotope stages numbered, natural remanent magnetization (NRM) after demagnetization at peak fields of 20 mT and 80 mT, volume magnetic susceptibility, isothermal remanence (IRM) and anhysteretic remanence (ARM), both remanences after demagnetization at peak fields of 35 mT. Magnetic measurements on u-channel samples.

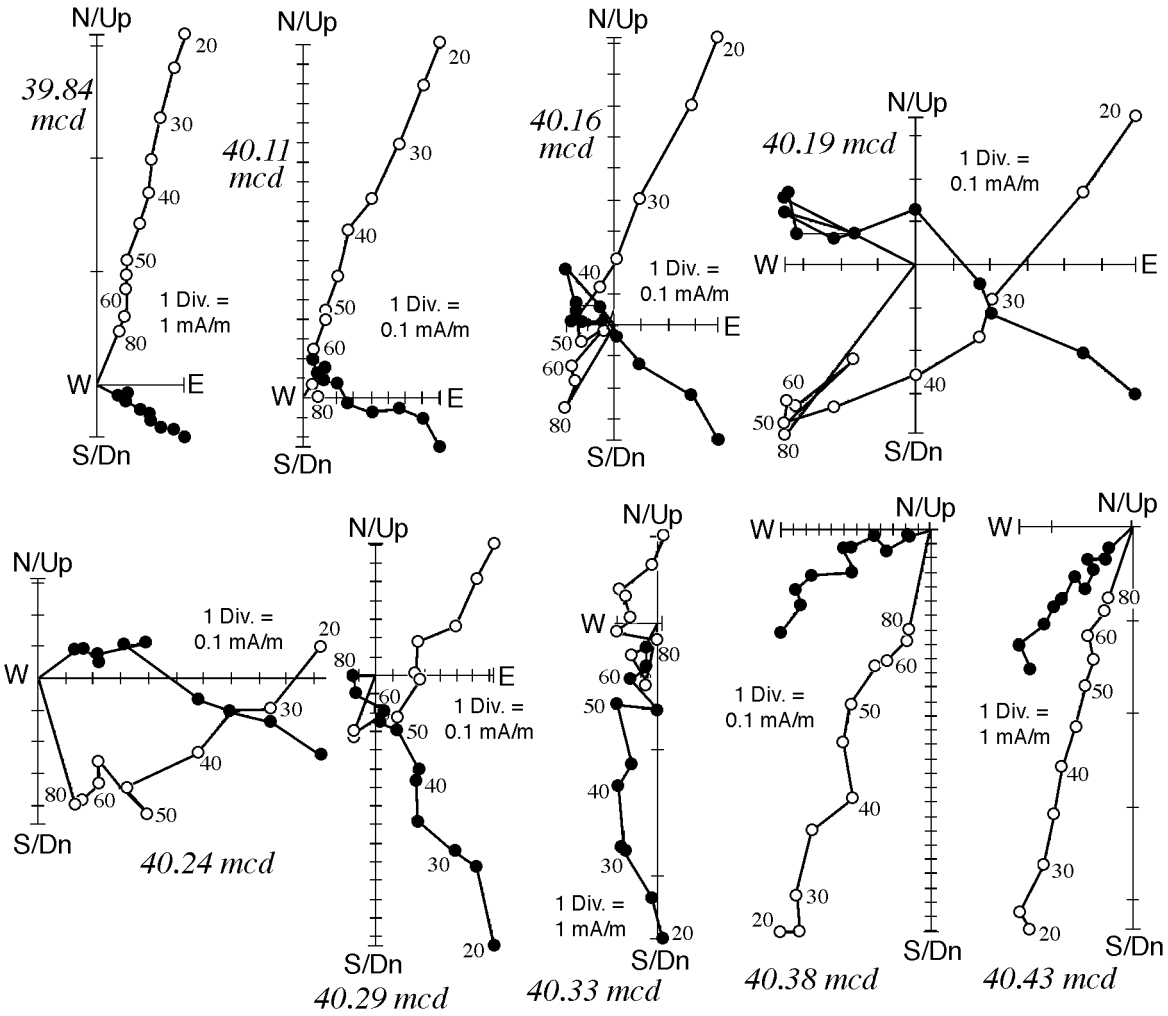

Figure 3. Orthogonal projection of alternating field demagnetization data for samples from the polarity reversal at the top of the Olduvai Subchronozone at ODP Site 982. Superimposed magnetization components are apparent in the 22 cm transition interval (40.11–40.33 mcd). Representative projections are shown. Data acquired at stratigraphic interval of 1 cm on u-channel samples with a magnetometer response function width of ~3.5 cm. Open and closed symbols indicate projection on the vertical and horizontal planes, respectively. The positions of the samples in meters composite depth (mcd) are indicated. The peak alternating fields range from 20 mT to 80 mT.

[1990, 1995a,b] as defined by his TARGET curve (http://delphi.esc.cam.ac.uk/coredata/v677846.html) shown in Figure 3. Depth/age tie points are given in Table 1. The TARGET curve in the interval of interest comprises data from ODP Site 677 (0.34–1.81 Ma) and ODP Site 846 (1.81–2.70 Ma) [*Shackleton et al*., 1990; 1995a,b]. In Figure 3, the match of the Site 982 $\delta^{18}O$ record with the TARGET curve is compared with the benthic $\delta^{18}O$ record from DSDP Site 607 [*Raymo et al*., 1989] which was independently correlated to the Shackleton time scale used here. Note that the Site 982 age model of Venz et al. [1999], subsequently used by Flower et al. [2000] and Kleiven et al. [2003], utilizes a different target curve and hence differs slightly from the age model used here. The age model for ODP Site 980/981 [*Channell and Raymo*, 2003; *Channell et al*., 2003] utilizes the same TARGET curve used here for Site 982.

3.MAGNETIC MEASUREMENTS

Magnetic remanence and susceptibility measurements were made on u-channel samples (with 2x2 cm square cross-sections) collected from the archive half of the Site 982 composite section in the 7–66 mcd interval. Magnetic remanence measurements were made using a pass-through 2G magne-

Table 1. Depth/age tie-points for ODP Site 982

mcd	ka	mcd	ka	mcd	ka
6.87	336.0	30.05	1251.0	47.69	2153.0
8.39	370.0	30.55	1290.0	47.80	2162.1
9.84	408.0	31.90	1365.0	48.00	2179.6
14.19	531.0	34.10	1461.0	48.35	2192.0
16.15	630.0	35.25	1542.0	48.80	2243.0
17.78	678.3	37.73	1653.0	49.50	2282.0
19.18	750.0	38.48	1701.0	50.78	2363.0
20.53	798.0	39.03	1730.0	52.18	2441.0
22.58	873.0	40.40	1788.0	52.53	2465.0
24.58	966.0	41.60	1875.0	53.28	2486.0
26.13	1041.0	42.45	1916.0	53.73	2507.0
26.43	1050.0	44.15	1988.0	54.58	2525.0
26.68	1060.0	44.85	2045.0	55.28	2543.0
27.68	1098.0	45.80	2084.0	56.63	2579.0
28.35	1131.0	47.45	2137.9	57.33	2597.0
29.20	1197.0	47.65	2144.2	58.00	2642.0

tometer designed for u-channel samples [see *Weeks et al*., 1993]. Volume magnetic susceptibility measurements utilized a u-channel track incorporating a Sapphire Instruments 3.5 cm-square susceptibility loop [*Thomas et al*., 2003]. Shipboard treatment of archive halves of the composite section involved AF demagnetization of natural remanent magnetization (NRM) at maximum peak fields of 25 mT [*Channell and Lehman*, 1999]. Subsequent treatment of NRM on u-channel samples constituted alternating field (AF) demagnetization at peak fields of 20 to 60 mT (5 mT steps), 70 mT and 80 mT. The natural remanent magnetization (NRM) intensity falls by an order of magnitude between the 20 mT and 80 mT demagnetization steps (Figure 2) indicating that the NRM is carried by a low coercivity mineral such as magnetite. Thermal demagnetization of isothermal remanent magnetization and hysteresis ratios at neighboring sites (ODP Sites 980/981, 983 and 984) indicate pseudo-single domain (PSD) magnetite as the principal remanence carrier in the sediment drifts of the Iceland Basin [*Channell et al*., 1997, 1998; *Channell*, 1999; *Channell and Raymo*, 2003].

Orthogonal projections of AF demagnetization data from ODP Site 982 indicate the presence of a well-defined, low coercivity, magnetization component (e.g. samples at 39.84 mcd and 40.43 mcd in Figure 3). In the immediate vicinity of polarity zone boundaries, multi-component magnetizations are occasionally observed. For example, at the top of the Olduvai Subchronozone in the 40.11–40.33 mcd interval (Figure 3), a lower coercivity post-reversal magnetization appears to be superimposed on a higher coercivity pre-reversal magnetization.

Component declination and inclination were computed from u-channel data by applying the standard least squares method [*Kirschvink*, 1980] to the 20–70 mT demagnetization interval. The demagnetizaton interval was modified for some samples at polarity zone boundaries (e.g. those at 40.19 and 40.24 mcd in Figure 3). Maximum angular deviation (MAD) values are less than 10° for the majority of the magnetization components (Figure 4). Component declination and inclination define a polarity stratigraphy from the mid-Brunhes Chronozone to the Gauss Chronozone (Figure 4).

Anhysteretic remanence (ARM) was applied to u-channel samples using 100 mT AF and a 0.05 mT DC field. The ARM was measured and then progressively demagnetized in the same steps applied to the NRM. ARM intensity, after AF demagnetization in peak fields of 35 mT, varies over a range of 0.1 to 0.6 A/m in the 7 to 55 mcd interval (Figure 2). ARM values are close to zero below 55 mcd where carbonate percentages reach 90% [*Ortiz et al*., 1999]. A similar trend is observed for isothermal remanence (IRM), applied in a 500 mT DC field (Figure 2). Anhysteretic susceptibility (k_{arm}), the ARM normalized by the biasing DC field, divided by volume susceptibility (k) can be used as a measure of magnetite grain size [*King et al*., 1983]. For ODP Site 982, the k_{arm}/k ratios (Figure 5) imply magnetite grain sizes of <0.1 μm for low susceptibility intervals (full interglacial stages) and grain sizes of ~1–5 μm for high susceptibility intervals (full glacial stages).

Volume susceptibility, ARM and IRM fluctuate by more than an order of magnitude, particularly below 45 mcd (Figure 2). In order to test the coercivity match of NRM to ARM and IRM, and evaluate the potential for deriving paleointensity proxies, we plot the slope of NRM versus ARM (or IRM) in the 25–45 mT demagnetization range (Figure 6b). In ideal circumstances, the slopes constitute paleointensity proxies and the linear correlation coefficients (r) associated with the slopes should be close to unity. In the vicinity of the Matuyama-Brunhes boundary (Figure 6), the linear correlation coefficients depart significantly from unity. This indicates that neither IRM nor ARM have coercivity that matches that of NRM in this interval. For the 900–1700 ka (22–38 mcd) interval, however, linear correlation coefficients are usually above 0.9 indicating that the coercivity of NRM matches the coercivity of IRM and ARM. This is also the interval over which the values of IRM and ARM are less variable (Figure 2).

The paleointensity proxy derived from the slope of NRM/ARM can be compared with other records for the 900–1700 ka interval. In Figure 7, we compare the ODP Site 982 normalized remanence record with the paleointensity records from the Ontong-Java Plateau [*Kok and Tauxe*, 1999], the California Margin [*Guyodo et al*., 1999], the Equatorial Pacific [*Valet and Meynadier*, 1993; *Meynadier et al*., 1995], and ODP Sites 983/984 [*Channell and Kleiven*, 2000; *Channell et al*., 2002]. Mean sedimentation rates in the Matuyama

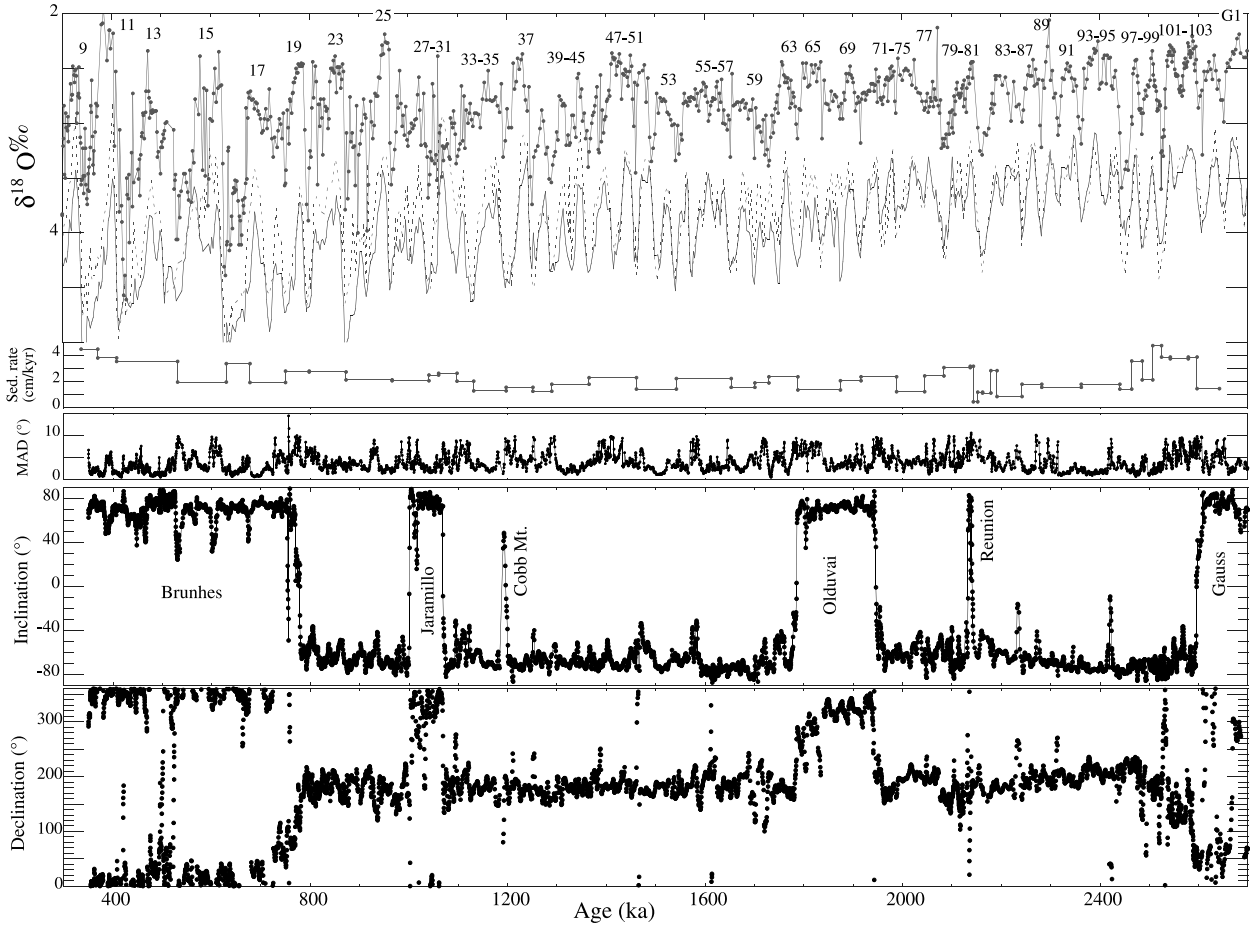

Figure 4. ODP Site 982: Benthic $\delta^{18}O$ data versus age from ODP Site 982 (fine line with points) compared to the chronology of Shackleton et al. [1990] as defined by his TARGET curve(http://delphi.esc.cam.ac.uk/coredata/v677846.html) (fine continuous line) and benthic $\delta^{18}O$ data from DSDP Site 607 [*Raymo et al*., 1989] (dashed line) tuned to the same TARGET curve. The TARGET curve comprises data from ODP Sites 677 (0.34–1.81 Ma) and 846 (1.81–2.70 Ma) [*Shackleton et al*., 1990; 1995a,b]. Interval sedimentation rates according to the age model, maximum angular deviation (MAD) values associated with component magnetization directions, component inclinations and declinations placed on the oxygen isotope age model.

Chronozone are ~2 cm/kyr or less for all records in Figure 7, apart from ODP Sites 983/984 where mean sedimentation rates are ~15 cm/kyr. To compensate for differing sedimentation rates, the ODP Site 983/984 records in Figure 7 have been smoothed using a 10 kyr running mean.

Some offsets in Figure 7 can be explained by discrepancies in chronology. The Ontong-Java stack was dated by linear interpolation between polarity reversals at the Matuyama-Brunhes boundary (MBB), the boundaries of the Jaramillo Subchronozone, and the Gauss-Matuyama boundary [*Kok and Tauxe*, 1999]. The age control at ODP Site 1021 (California Margin) for the Matuyama Chronozone was based on linear interpolation from the MBB to the boundaries of the Jaramillo Subchronozone [*Guyodo et al*., 1999]. The age control for the Equatorial Pacific ODP Leg 138 record [*Valet and Meynadier*, 1993; *Meynadier et al*., 1995] was based on orbital tuning of the GRAPE density stratigraphy [*Shackleton et al*., 1995a]. The age models for ODP Sites 983/984 [*Channell and Kleiven*, 2000; *Channell et al*., 2002] were derived by tuning to the Ice Volume Model of Imbrie and Imbrie [1980] for the 700–1100 ka interval, and by matching the $\delta^{18}O$ and susceptibility records to the ODP Site 677 $\delta^{18}O$ record [*Shackleton et al*., 1990] for the older part of the record.

Paleointensity lows at ~990 ka, 1070 ka and 1200 ka in Figure 7 correspond to the boundaries of the Jaramillo Subchron (TJ/BJ) and to the Cobb Mountain Subchron (C). The normalized remanence record from ODP Site 982 for the 900–1600 ka interval can be matched to paleointensity records

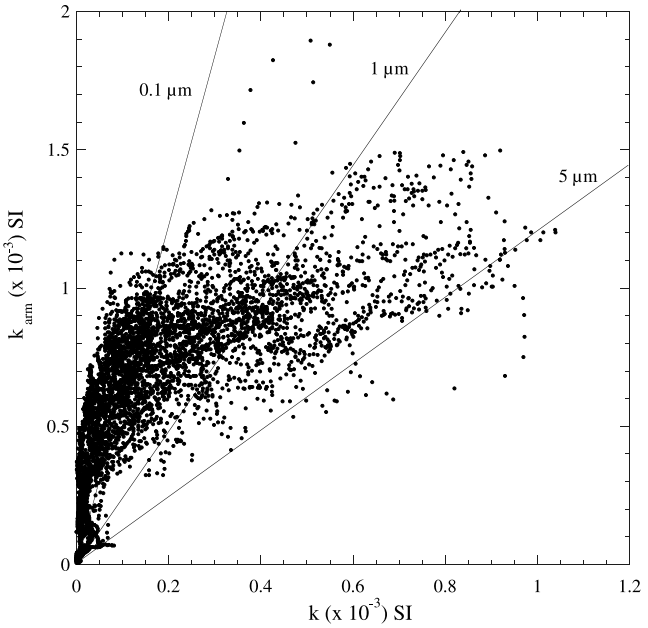

Figure 5. Anhysteretic susceptibility (k_{arm}), the ARM normalized by the biasing DC field, plotted against volume susceptibility (k) for ODP Site 982. Magnetite grain size estimates from King et al. [1983].

from the Iceland Basin (ODP Sites 983/984) and to records from the Pacific Ocean (Figure 7). The Equatorial Pacific record and the Site 983/984 records are better aligned with the Site 982 record than the California Margin and Ontong-Java records (Figure 7). This reflects the enhanced age control for the Equatorial Pacific record and for ODP Sites 982/983/984 as outlined above. Paleointensity lows correspond to the boundaries of the Jaramillo Subchronozone (TJ/BJ), the Santa Rosa excursion (SR), the Punaruu excursion (P) [*Singer et al*., 1999], the Cobb Mountain excursion (C) [*Clement and Kent*, 1987], the Ontong-Java excursion (OJ) [*Valet and Meynadier*, 1993; *Gallet et al*., 1993], the Gardar excursion (Ga) [*Channell et al*., 2002] and the Gilsa excursion (Gi) [*Clement and Kent*, 1987; *Channell et al*., 2002].

4. REVERSAL AGE OFFSETS AT SITES 980–982

The correlations of Pliocene-Pleistocene isotopic stages to polarity chrons and subchrons at ODP Site 982 are consistent with correlations established elsewhere (Table 2). The magnetic and $\delta^{18}O$ data from Site 982 and from neighboring Site 980/981 (Figure 1) are sufficiently detailed to allow an assessment of the precise position of reversals relative to isotopic stages. Mean sedimentation rates at Site 982 and Site 980/981 differ by factors of 2–7, and hence the precise correlation of reversals to isotopic stages at these sites may give insights into the magnetization lock-in function. Mean sedimentation rates in the Matuyama Chron at Site 982 vary in the 1–3 cm/kyr range (Figure 4). At Site 980/981, mean sedimentation rates in the Matuyama Chron vary in the 5–30 cm/kyr range [*Channell and Raymo*, 2003; *Channell et al*., 2003].

The age models at Site 982 and Site 980/981 were derived by matching the benthic $\delta^{18}O$ records to the same TARGET curve (see above). For the two sites, the ages of polarity reversals at the boundaries of the Jaramillo Chronozone, the Cobb Mountain Subchronozone, the Olduvai Subchronozone and the Réunion Subchronozone are discrepant by 10–15 kyr (Figure 8). With the exception of the base of the Réunion Subchronozone (Figure 8d), the ages of polarity reversals appear older for Site 982, the site with lower mean sedimentation rates. This could be explained by incorrect correlation of the $\delta^{18}O$ records to the TARGET curve and inadequacy of the age model. For example, the Site 982 $\delta^{18}O$ records at the boundaries of the Jaramillo Chronozone lack distinctive features (Figure 8a), and may therefore be misaligned with the TARGET curve. The consistent age offset, however, with older ages for Site 982, tends to indicate that the offset is related to the magnetization lock-in function. If the physical lock-in functions were comparable for the two neighboring sites, the lock-in *time* would have been more extended for the site with the lower sedimentation rates. The modeling of this process, developed below, indicates that lock-in depth for the lower sedimentation rate site (Site 982) must have been greater to account for the observed age offsets.

Post-depositional remanent magnetization (pDRM), stemming from the work of Irving and Major [1964], has been modeled by an exponential function [*Hyodo*, 1984; *Meynadier and Valet*, 1996; *Mazaud*, 1996; *Teanby and Gubbins*, 2000; *Guyodo and Channell*, 2002]. Teanby and Gubbins [2000] added an 8 cm uniform mixing layer (magnetization = 0) at the top of the sedimentary column to simulate the bioturbated surface mixed layer. The assumption of a well-mixed layer, in which the sediment is consumed by organisms such as sipunculid or echiuran worms, is valid in deep-sea sediments where the mixing coefficient exceeds the product of mixed layer depth and sedimentation rate [*Guinasso and Schink*, 1975]. In deep-sea sediments, isotopic tracers indicate mean mixed layer thicknesses of about 10 cm (values vary by an order of magnitude from 3–30 cm) that is largely independent of sedimentation rate [*Boudreau*, 1994, 1998]. The main control on the mixed-layer thickness appears to be organic carbon flux derived from surface water productivity [*Trauth et al*., 1997; *Smith and Rabouille*, 2002]. We would, therefore, expect the mixed layer thickness at Site 982, with its lower detrital component and higher organic carbon flux, to exceed that at Site 980/981. Using ^{14}C of the bulk carbonate fraction as the isotopic tracer, Thomson et al. [2000] estimated mixed-layer thicknesses of 10–20 cm in box cores col-

lected close to the Rockall Plateau at water depths comparable to Sites 980–982. These values are greater than the 2–13 cm mixed-layer thicknesses obtained from further south in the North Atlantic using ^{14}C in foraminifera [*Trauth et al*., 1997; *Smith and Rabouille*, 2002]. Estimates of mixed-layer thickness are grain-size sensitive [see *Bard*, 2001] and would be expected to be lower for the coarse fraction (foraminifera) than for the bulk carbonate (nannofossils). For this reason, mixed layer thickness estimates based on ^{14}C and other isotopic tracers should be considered as minimum estimates for the fine (PSD) grains that carry stable magnetization. In the studies of Thomson et al. [2000] and Trauth et al. [1997], uni-

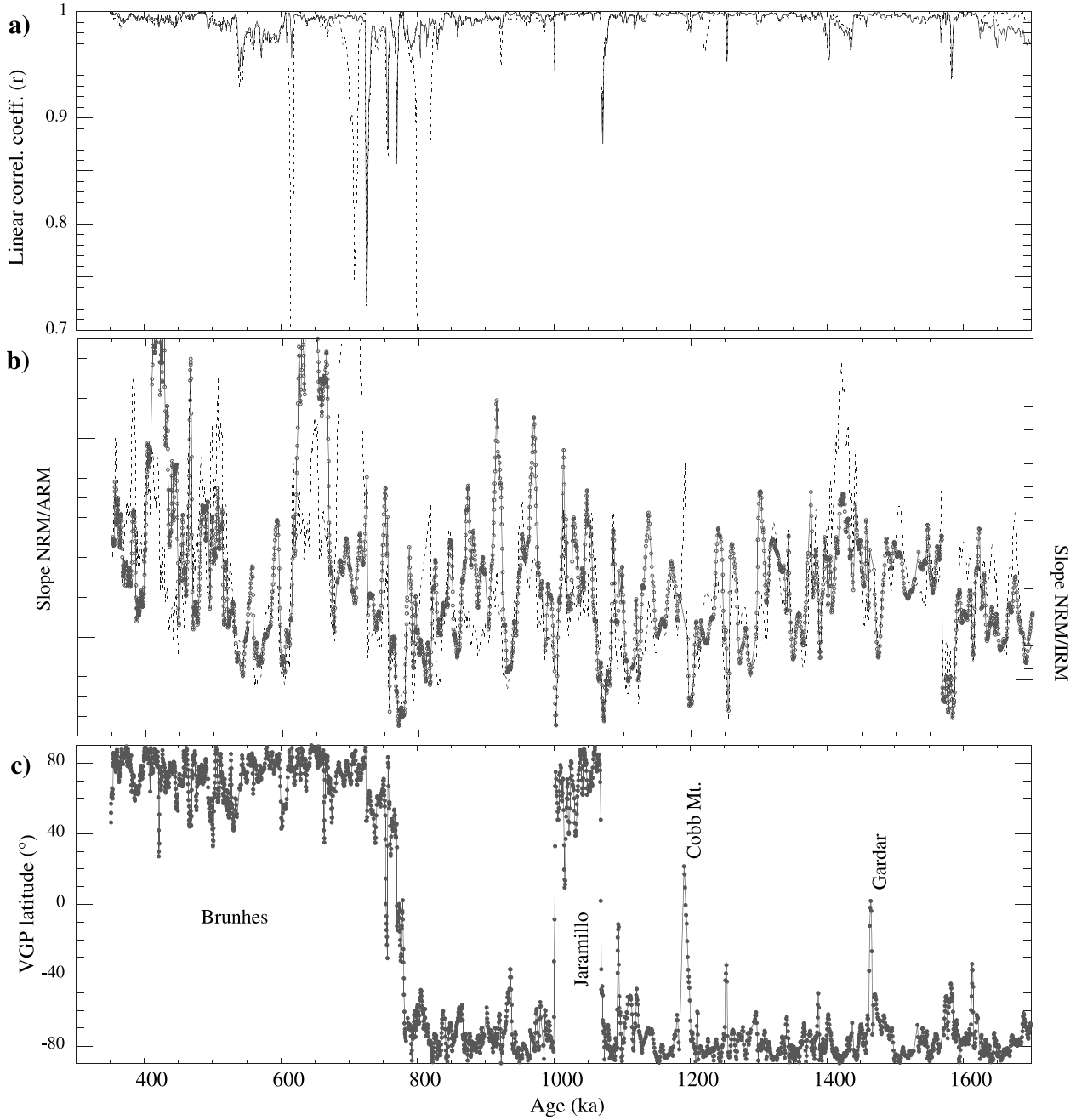

Figure 6. ODP Site 982: Linear correlation coefficients (r) and slopes of NRM versus ARM (solid line) and NRM versus IRM (dashed line) for the 25–45 mT peak field range in the 300–1700 ka interval. Virtual geomagnetic polar (VGP) latitudes derived from the component directions in Figure 4.

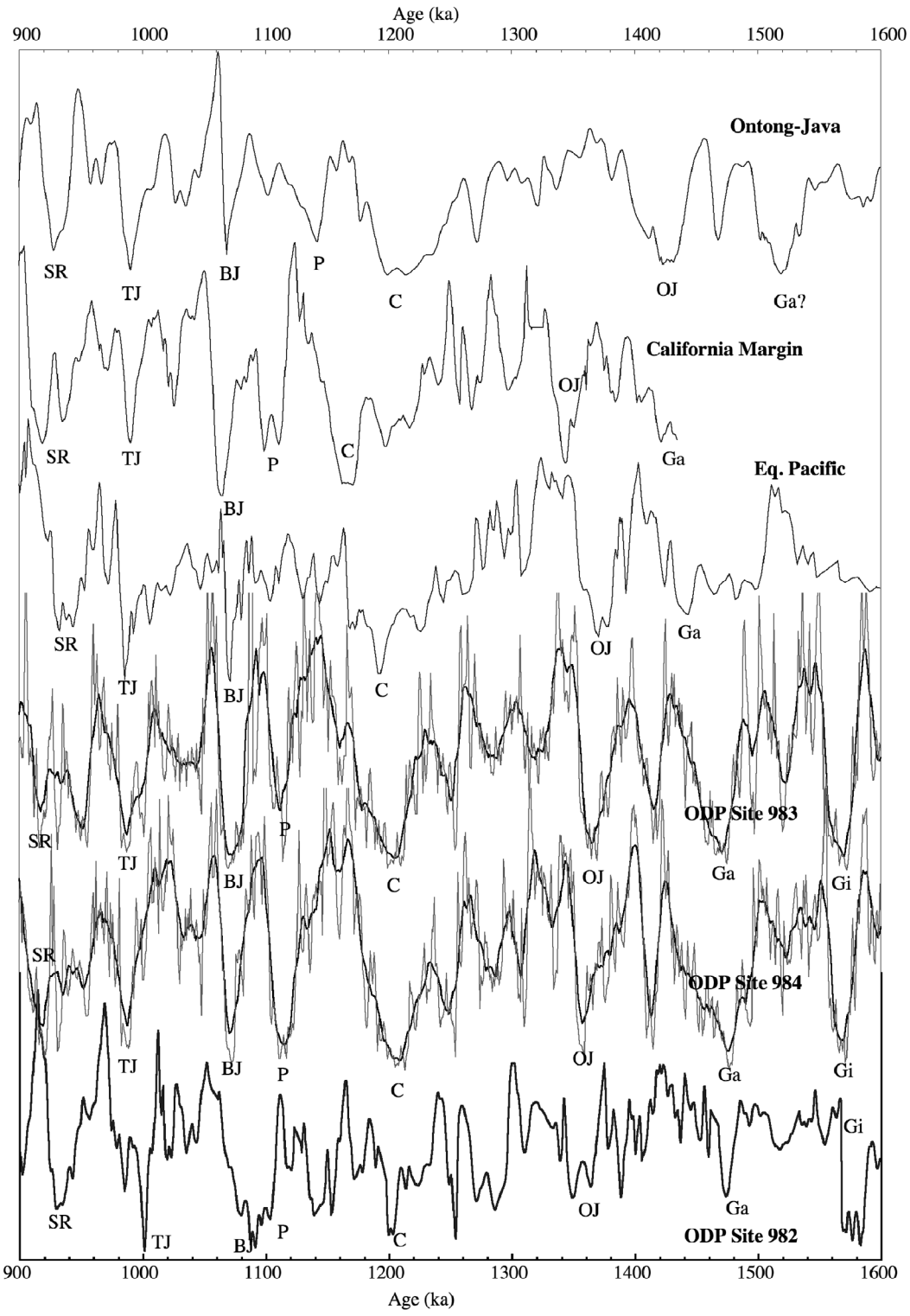

Figure 7. Comparison of NRM/ARM (slope) for ODP Site 982 with paleointensity data from Ontong-Java Plateau [*Kok and Tauxe*, 1999], California Margin [*Guyodo et al*., 1999], Equatorial Pacific [*Valet and Meynadier*, 1993; *Meynadier et al*., 1995], and from ODP Sites 983 and 984, before and after smoothing with a 10 kyr running mean [*Channell and Kleiven*, 2000*; Channell et al*., 2002].

Table 2. Positions of reversals and polarity subchronozones relative to marine isotope stages (MIS)

Subchronozone	Subchron label*	MIS[1] Sites 607, 609, 677	MIS[2] Italy	MIS[3] Site 980/981	MIS[4] Site 983	MIS[4] Site 984	MIS Site 982 (this paper)
top Jaramillo	end 1r.1n	mid 27	27	mid 27	mid 27	mid 27	base 27
base Jaramillo	onset 1r.1n	mid 31	31	top 31	mid 31	mid 31	mid 31
Punaruu	1r.2r.1r				base 33	base 33	base 33
top Cobb. Mt.	end 1r.2r.2n	base 35		mid 35	mid 35	mid 35	base 35
base Cobb Mt.	onset 1r.2r.2n	base 35		base 35	mid 36	mid 36	base 35
top Olduvai	end 2n	base 63	64	63	base 63	base 63	base 63
base Olduvai	onset 2n	base 71	72	top 71		base 71	71
Réunion	2r.1n	79-80	81	79-81		base 81	81

MIS: marine isotope stage

* [nomenclature of *Cande and Kent*, 1992]

[1] [*Ruddiman et al.,* 1989; *Raymo et al.,* 1989; *Shackleton et al.,* 1990]

[2] [*Lourens et al.,* 1996]

[3] [*Channell and Raymo*, 2003; *Channell et al*., 2003]

[4] [*Channell et al.,* 2002]

form ^{14}C values in the mixed layer, and an abrupt change to uniformly increasing ^{14}C ages below, imply that the mixing coefficient (efficiency) is high in the mixed layer on millennial (^{14}C) timescales.

A simple way of explaining the age offsets observed between Site 982 and Site 980/981 would be to consider a larger surface mixed layer at Site 982. In view of the observed average age offset and the difference in average sedimentation rates between the two sites, an increased mixed layer thickness of about 25 cm would be required. In order to study this problem in a more comprehensive manner, we consider a number of parameters: (1) estimated interval sedimentation rates, (2) age control procedures, (3) offsets due to magnetization lock-in, and (4) sample measurement effects. Rather than using a mixed layer (magnetization = 0) overlying an exponential lock-in function [*Teanby and Gubbins*, 2000], we have used a sigmoidal pDRM function based on tanh(x) (Figure 9a). This function has the attribute of describing a smooth transition between the mixing zone and the lock-in zone. The function can be defined by a surface mixing layer depth (M) at which 5% of the magnetization is acquired, and a lock-in depth (L) that is the depth below M at which 50% of the magnetization is acquired (Figure 9a). With this pDRM function, increasing M by *x* centimeters leads to an increase (by *x* cm) in the depth at which the magnetization is locked. An increase in L also leads to an increase in the depth at which the magnetization is locked but, more importantly, it leads to a marked increase in the depth interval over which the reversal transition is recorded (Figure 9a). Increasing L also reduces the time resolution of the record, as the lock-in function acts as a filter [*Teanby and Gubbins*, 2000; *Guyodo and Channell*, 2002].

The modeling procedure involved the following steps: (1) conversion from the time domain to the depth domain of a model virtual geomagnetic polar (VGP) latitude time series using sedimentation rate estimates from the age model, (2) simulation of the magnetization (pDRM) acquisition process, (3) simulation of the smoothing inherent in the u-channel measurement procedure, and (4) conversion back into the time domain.

The input VGP latitude time series was constructed as a step function representing a succession of reversals corresponding to the onset and termination of Jaramillo, Cobb Mountain, Olduvai, and Réunion subchrons. The initial duration of the reversals was set to 4 kyr, based on the distribution of reversal durations obtained from ODP Sites 983 and 984 [*Channell et al*., 2002]. For each simulation, the age-scale of this initial time series was converted to a depth-scale using the sedimentation rates specific to each site investigated (Figure 8). The magnetization acquisition process was subsequently simulated as a convolution between this input signal and the pDRM function described above. In this function, both L and M can be varied systematically in order to define the curve that will best fit the real data (i.e., yield the appropriate mid-reversal position and transition duration). A more precise fit would require simulation of the details of each reversal record, including the (amplified) secular variation during reversal transitions. Note that the mixing depth necessary to match the real data depends on the initial age chosen for the reversals. Since the precise absolute age of reversals is not known with sufficient accuracy, the position of the reversals in the model signal was arbitrarily fixed at some time before the occurrence of the reversals in the real data. Using this method, only relative values of the mixing depth between sites (hereafter referred to as DM) could be obtained for a given input. Subsequently, another function was applied to simulate the smoothing introduced by the magnetometer during measurement of the u-channel. This func-

tion was chosen as the *z axis* response function of the 2-G Enterprises cryogenic magnetometer located at the University of Florida [*Guyodo et al*., 2002]. The resulting signal was then converted back into the time domain using site-specific sedimentation rates.

Using this approach, the observed reversal offsets (Figure 8) can be simulated by values of DM ($M_{Site\ 982} - M_{Site\ 980/981}$) of ~20 cm for the boundaries of the Jaramillo and for the Cobb Mt. (Figure 9b), 16 cm for the base of the Olduvai and 36 cm for the top of the Réunion (Figure 9c). High values of L do not generate the desired offset but extend the apparent duration of the polarity reversal (Figure 9a). Values of L < 10 cm appear to satisfy the observations (Figures 9 b,c). Evidently, this value depends to some extent on the duration chosen for the initial reversals (here 4 kyr), and therefore could vary by a few centimeters. Large fluctuations in sedimentation rates at the onset of the Olduvai Subchron and within the Réunion Subchron make the results of these simulations more problematic than the estimates for the boundaries of the Jaramillo and Cobb Mt. subchrons. Indeed, a slight change

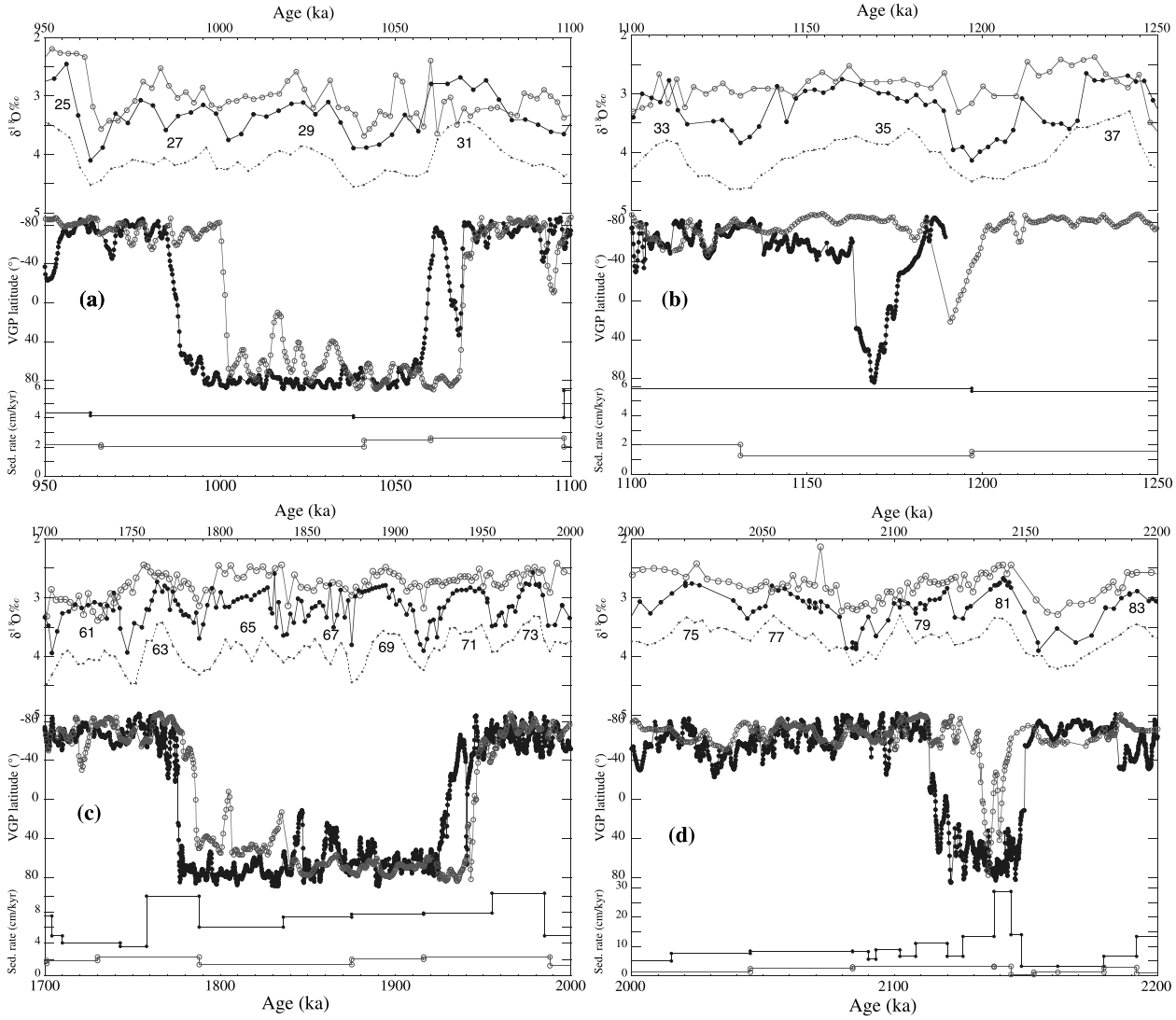

Figure 8. Comparison of Site 982 and Site 980/981. (a) Jaramillo Subchronozone, (b) Cobb Mountain Subchronozone, (c) Olduvai Subchronozone, (d) Reunion Subchronozone. Benthic $\delta^{18}O$ with marine isotope stage numbers for Site 982 (thin line, open symbols) and Site 980/981 (thick line, closed symbols) correlated to the TARGET curve (dashed line) from Shackleton et al. [1990, 1995a,b]. Virtual geomagnetic polar latitudes (VGPs) from Site 982 (thin line, open symbols) and Site 980/981 (thick line, closed symbols). Sedimentation rates for Site 982 (thin line, open symbols) and Site 980/981 (thick line, closed symbols).

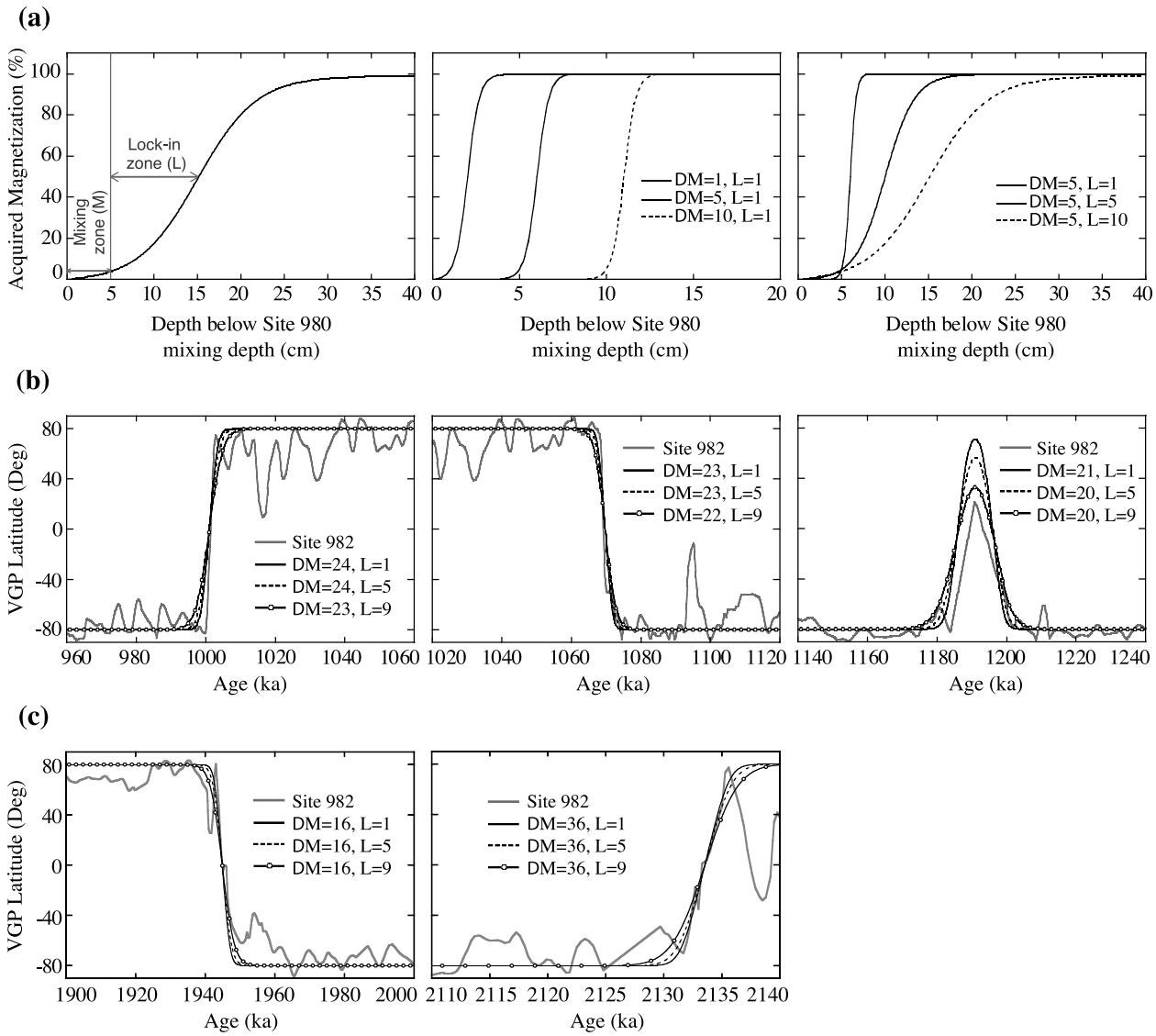

Figure 9. (a) The sigmoidal function based on tanh(x) used to model the mixing zone (thickness M) and the underlying lock-in zone (thickness L). The effect of varying the difference in mixing zone depth (DM) between Sites 982 and 980/981, and lock-in depth (L), is illustrated. The sigmoidal function can be used to model the reversal offsets between the two sites for (b) the boundaries of the Jaramillo and Cobb Mt. subchronozones and (c) the base of the Olduvai and top of the Réunion subchronozones.

in the positioning of a reversal (in the input signal) relative to the boundary between two different sedimentation rate intervals (i.e., an age model tie-point), may place this reversal either in a higher or a lower sedimentation rate interval, which will alter the model output.

5. DISCUSSION

A recent re-deposition study has suggested that, at least for some lithologies, inter-granular interaction could reduce significantly the extent of pDRM, and bioturbation would not enhance, but rather disrupt, the remanent magnetization below the sediment/water interface [*Katari et al*., 2000]. The conclusions of this paper are consistent with studies by Tauxe et al. [1996], based on a comparison of magnetic and oxygen isotope records at the MBB, that imply that magnetization lock-in depth is insignificant in these (low sedimentation rate) marine sediments. Other studies [*DeMenocal et al*., 1990; *Lund and Keigwin*, 1994; *Kent and Schneider*, 1995] invoked pDRM, and hence a finite lock-in depth, to explain rever-

sal/isotope offsets, and observed attenuation of secular variation records.

At Sites 982 and 980/981, the consistent sense of age offset of reversals between Sites 982 and 980/981 can, according to the model presented above, be explained by a mixing depth (zone) that is significantly thicker (by ~20 cm) at Site 982 than at Site 980/981. The simulations imply that magnetization is acquired very soon after the sediment passes through the mixed layer (M), the lock-in layer (L) beneath the mixed layer being just a few centimeters thick. Estimates of mixed layer thickness, based on ^{14}C, from Holocene pelagic sediments in the eastern North Atlantic give mixed layer thicknesses of ~2–20 cm [*Thomson et al*., 2000; *Trauth et al*., 1997]. Large variations in M are found for pelagic sediments, with no clear dependence on sedimentation rate [*Boudreau*, 1994, 1998]. Lower mean sedimentation rates at Site 982, relative to Site 980/981 (Figure 8), do not imply that the mixed layer depth (M) would be greater at Site 982 than at Site 980/981. Organic carbon flux is believed to be a control on mixed layer thickness [*Trauth et al*., 1997; *Smith and Rabouille*, 2002]. Higher carbonate content (lower detrital concentration) and shallower water depth at Site 982, relative to Site 980/981, implies that organic carbon flux to the seafloor was greater for Site 982 than for Site 980/981. The higher organic carbon flux at ODP Site 982 may, therefore, account for the larger surface-sediment mixed-layer thickness at ODP Site 982.

The difference in mixed layer thickness between the two sites is proposed as an explanation for the apparent age offset of reversals in the Matuyama Chron. It is important to note that this difference in mixed layer thickness would affect the $\delta^{18}O$ record, and hence the age model. The small number of foraminifera (1–3) required by modern mass spectrometers for precise estimates of $\delta^{18}O$ has exacerbated the effect of reworking on $\delta^{18}O$ records in general. Reworking down-section is limited by the extent of the mixed layer, but no such limitation exists for reworking up-section [see *Guinasso and Schink*, 1975]. As a result of lower sedimentation rates and larger mixing layer thickness at Site 982, the definition of the isotope stratigraphy (and hence the age model) would be reduced at Site 982 relative to that at Site 980/981. Mixed layer effects on the isotopic data should be taken into account in future, more comprehensive simulations. Nevertheless, it is very unlikely that reworking and fortuitous picking of specimens would offset the Site 982 $\delta^{18}O$ record to account for the observed offsets in ages of polarity reversals.

Acknowledgments. Research supported by US National Science Foundation (EAR-98-04711). We are indebted to the staff of the Ocean Drilling Program (ODP) for facilitating this study, particularly the staff at the ODP Bremen Core Repository. We thank Chris Bayliss for careful laboratory measurements. The paper benefited from discussions with Kathy Venz-Curtis and John Jaeger, and from the comments of three anonymous reviewers.

REFERENCES

Bard, E., Paleoceanographic implications of the difference in deep-sea sediment mixing between large and fine particles, *Paleoceanography*, 16, 235–239, 2001.

Boudreau, B. P., Is burial velocity a master parameter for bioturbation?, *Geochim. Cosmochim. Acta*, 58, 1243–1249, 1994.

Boudreau, B. P., Mean mixing depth of sediments: The wherefore and the why, *Limnol. Oceanogr*., 43, 524–526, 1998.

Cande, S. C., and D. V. Kent, A new geomagnetic polarity timescale for the late Cretaceous and Cenozoic, *J. Geophys. Res*. 97, 13917–13951, 1992.

Channell, J .E. T., D. A. Hodell and B. Lehman, Relative geomagnetic paleointensity and $\delta^{18}O$ at ODP Site 983 (Gardar Drift, North Atlantic) since 350 ka, *Earth Planet. Sci. Lett*., 153, 103–118, 1997.

Channell, J. E. T., D. A. Hodell, J. McManus and B. Lehman, Orbital modulation of geomagnetic paleointensity, *Nature*, 394, 464–468, 1998.

Channell, J. E. T., and B. Lehman, Magnetic stratigraphy of Leg 162 North Atlantic Sites 980–984, In: Jansen, E., Raymo, M.E., Blum, P. and Herbert, T. (Eds.), *Proc. ODP, Sci. Results*, 162: College Station, TX (Ocean Drilling Program), 113–130, 1999.

Channell, J. E. T. and H. F. Kleiven, Geomagnetic palaeointensities and astrochronological ages for the Matuyama-Brunhes boundary and the boundaries of the Jaramillo Subchron: palaeomagnetic and oxygen isotope records from ODP Site 983, *Phil. Trans. R. Soc. Lond*. A, 358, 1027–1047, 2000.

Channell, J. E. T. and M. E. Raymo, Paleomagnetic record at ODP Site 980 (Feni Drift, Rockall) for the past 1.2 Myrs, *Geochem., Geophys. Geosyst*., doi:10.1029/2002GC000440, 2003.

Channell, J. E. T., A. Mazaud, P. Sullivan, S. Turner, and M. E. Raymo, Geomagnetic excursions and paleointensities in the 0.9–2.15 Ma interval of the Matuyama Chron at ODP Site 983 and 984 (Iceland Basin), *J. Geophys. Res*., 107 (B6), 10.1029/2001JB000491, 2002.

Channell, J.E.T., J. Labs, and M. E. Raymo, The Réunion Subchronozone at ODP Site 981 (Feni Drift, North Atlantic), *Earth Planet. Sci. Lett*., 215, 1–12, 2003.

Clement, B. M., and D. V. Kent, Short polarity intervals within the Matuyama: transition field records from hydraulic piston cored sediments from the North Atlantic, *Earth Planet. Sci. Lett*., 81, 253–264, 1987.

DeMenocal, P. B., W. F. Ruddiman, and D. V. Kent, Depth of post-depositional remanence acquisition in deep-sea sediments: a case study of the Brunhes-Matuyama reversal and oxygen isotopic stage 19.1, *Earth Planet. Sci. Lett*., 99, 1–13, 1990.

Flower, B. P., D. W. Oppo, J. F. McManus, K. A. Venz, D. A. Hodell, and J. A. Cullen, North Atlantic intermediate to deep water circulation and chemical stratification during the past 1 Myr, *Paleoceanography*, 15, 388–403, 2000.

Gallet, Y., J. Gee, L. Tauxe and J. A. Tarduno, Paleomagnetic analyses of short normal polarity magnetic anomalies in the Matuyama

chron, In: Berger, W.H., Kroenke, L.W. and Mayer, L.A. (Eds.). *Proc. ODP Sci. Results*, 130: 547–559, 1993.

Guinasso, N. L. and D. R. Schink, Quantitative estimates of biological mixing rates in abyssal sediments, *J. Geophys. Res*., 80, 3032–3043, 1975.

Guyodo, Y. and J. E. T. Channell, Effects of variable sedimentation rates and age errors on the resolution of sedimentary paleointensity records, *Geochem., Geophys. Geosyst*., 10.1029/2001GC000211, 2002.

Guyodo, Y., C. Richter and J-P. Valet, Paleointensity record from Pleistocene sediments (1.4–0 Ma) off the California Margin, *J. Geophys, Res*., 104, 22,953–22,964, 1999.

Guyodo, Y., J. E. T. Channell, and R. G. Thomas, Deconvolution of u-channel paleomagnetic data near geomagnetic reversals and short events, *Geophys. Res. Lett*., 29, 1845, doi:10.1029/2002GL014927, 2002.

Hyodo, M., Possibility of reconstruction of the past geomagnetic field from homogeneous sediments, *J. Geomag. Geoelectr*., 36, 45–62, 1984.

Imbrie, J., and J. Z. Imbrie, Modeling the climatic response to orbital variations, *Science*, 207, 943–953, 1980.

Irving, E., and A. Major, Post-depositional detrital remanent magnetization in a synthetic sediment, *Sedimentology*, 3, 135–143, 1964.

Katari, K., L. Tauxe, and J. King, A reassessment of post-depositional remanent magnetism: preliminary experiments with natural sediments, *Earth Planet. Sci. Lett*., 183, 147–160, 2000.

Kent, D., and D. Schneider, correlation of paleointensity records in the Brunhes/Matuyama polarity transition interval, *Earth Planet. Sci. Lett*., 129, 135–144, 1995.

King, J. W., S. K. Banerjee, and J. Marvin, A new rock-magnetic approach to selecting sediments for geomagnetic paleointensity studies: application to paleointensity for the last 4000 years, *J. Geophys. Res*., 88, 5911–5921, 1983.

Kirschvink, J. L., The least squares lines and plane analysis of paleomagnetic data, *Geophys. J.R. Astr. Soc*. 62, 699–718, 1980.

Kleiven, H. F., E. Jansen, W. B. Curry, D. A. Hodell and K. Venz, Atlantic ocan thermohaline circulation changes on orbital to suborbital timescales during the mid-Pleistocene, *Paleoceanography*, 18, 1008, doi:10.1029/2001PA000629, 2003.

Kok, Y. S. and L. Tauxe, A relative geomagnetic paleointensity stack from Ontong-Java Plateau sediments for the Matuyama, *J. Geophys. Res*., 104, 25,401–25,413, 1999.

Lourens, L. J., A. Antonarakou, F. J. Hilgen, A. A. M. Van Hoof, C. Vergnaud-Grazzini and W. J. Zachariasse. Evaluation of the Plio-Pleistocene astronomical timescale, *Paleoceanography*, 11, 391–413, 1996.

Lund, S., and L. Keigwin, Measurement of the degree of smoothing in sediments paleomagnetic secular variation records: an example from late Quaternary deep-sea sediments of the Bermuda rise, western North Atlantic ocean, *Earth Planet. Sci. Lett*., 122, 317–330, 1994.

Manley, P. L. and D. W. Caress, Mudwaves on the Gardar Sediment Drift, NE Atlantic, *Paleoceanography*, 9, 973–988, 1994.

Mazaud, A., Sawtooth variation in magnetic intensity profiles and delayed acquisition of magnetization in deep sea cores, *Earth Planet. Sci. Lett*., 139, 379–386, 1996.

Meynadier, L., and J.-P. Valet, Post-depositional realignment of magnetic grains and asymetrical saw-toothed pattern of magnetization intensity, *Earth Planet. Sci. Lett*., 140, 123–132, 1996.

Meynadier, L., J-P. Valet, and N. J. Shackleton, Relative geomagnetic intensity during the last 4 M.Y. from the equatorial Pacific, In: Pisias, N. G., Janacek, L. A., Palmer-Julson, A., and Van Andel, T. H. (Eds.). *Proc. ODP Sci. Results*, 138: 779–793, 1995.

McCave, I. N., P. F. Lonsdale, C. D. Hollister and W. D. Gardner, Sediment transport over the Hatton and Gardar contourite drifts, *J. Sediment. Pet*., 50, 1049–1062, 1980.

Ortiz, J., A. Mix, S. Harris, and S. O'Connell, Diffuse spectral reflectance as a proxy for percent carbonate content in north Atlantic sediments, *Paleoceanography*, 14, 171–186, 1999.

Raymo, M. E., W. F. Ruddiman, J. Backman, B. M. Clement, and D. G. Martinson, Late Pliocene variation in Northern Hemisphere ice sheets and North Atlantic deep water circulation, *Paleoceanography*, 4, 413–446, 1989.

Ruddiman, W. F., M. E. Raymo, D. G. Martinson, B. M. Clement, and J. Backman, Pleistocene evolution: northern hemisphere ice sheet and north Atlantic ocean, *Paleoceanography*, 4, 353–412, 1989.

Schneider, D. A., Paleomagnetism of some Leg 138 sediments: detailing Miocene magnetostratigraphy, In: Pisias, N. G., Janacek, L. A., Palmer-Julson, A., and Van Andel, T. H. (Eds.). *Proc. ODP Sci. Results*, 138: 59–72, 1995.

Shackleton, N. J., A. Berger, and W. R. Peltier, An alternative astronomical calibration of the lower Pleistocene timescale based on ODP Site 677, *Trans. Roy. Soc. Edinburgh: Earth Sci*. 81, 251–261, 1990.

Shackleton, N. J., S. Crowhurst, T. Hagelberg, N. G. Pisias, and D. A. Schneider, A new Late Neogene time scale: application to Leg 138 Sites, In: Pisias, N. G., Janacek, L. A., Palmer-Julson, A., and Van Andel, T. H. (Eds.). *Proc. ODP Sci. Results*, 138: 73–101, 1995a.

Shackleton, N. J., M. A. Hall, and D. Pate, Pliocene stable isotope stratigraphy of Site 846, In: Pisias, N. G., Janacek, L. A., Palmer-Julson, A., and Van Andel, T. H. (Eds.), *Proc. ODP Sci. Results*, 138, 337–355, 1995b.

Shipboard Scientific Party, Site 982, In: Jansen, E., M. Raymo, P. Blum, et al., eds., *Proc. ODP Init. Repts*., 162: College Station, TX (Ocean Drilling Program), 91–138, 1996.

Singer, B. S., K. A. Hoffman, A. Chauvin, R. S. Coe, and M. S. Pringle, Dating transitionally magnetized lavas of the late Matuyama Chron: toward a new 40Ar/39Ar timescale of reversals and events, *J. Geophys. Res*., 104, 679–693, 1999.

Smith, C. R. and C. Rabouille, What controls the mixed-layer depth in deep-sea sediments? The importance of POC flux, *Limnol. Oceanogr*., 47, 418–426, 2002.

Tauxe, L., Sedimentary records of relative paleointensity of the geomagnetic field: theory and practice, *Rev. Geophys*., 31, 319–354, 1993.

Tauxe, L., J-P. Valet and J. Bloemendal, Magnetostratigraphy of Leg 108 advanced hydraulic piston cores, In: Ruddiman, W., Sarnthein et al. (Eds.). *Proc. ODP Sci. Results*, 108: 429–439, 1989.

Tauxe, L., T. Herbert, N. J. Shackleton, and Y. S. Kok, Astronomical calibration of the Matuyama-Brunhes boundary: consequences for the magnetic remanence acquisition in marine carbonates and Asian loess sequences, *Earth Planet. Sci. Lett*., 140, 133–146, 1996.

Teanby, N., and D. Gubbins, The effect of aliasing and lock-in processes on paleosecular variation records from sediments, *Geophys. J. Int*., 142, 563–570, 2000.

Thomas, R., Y. Guyodo and J.E.T. Channell, U-channel track for susceptibility measurements, *Geochem. Geophys. Geosyst*., 1050, doi: 10.1029/2002GC000454, 2003.

Thomson, J., L. Brown, S. Nixon, G.T. Cook and A.B. McKenzie, Bioturbation and Holocene sediment accumulation fluxes in the northeast Atlantic Ocean (Benthic Boundary Layer experiment sites), *Marine Geology*, 169, 21–39, 2000.

Tiedemann, R., M. Sarnthein and N.J. Shackleton, Astronomic timescale for the Pliocene Atlantic ?^{18}O and dust flux records of Ocean Drilling Program Site 659, *Paleoceanography*, 9, 619–638, 1994.

Trauth, M.H., M. Sarnthein and M. Arnold, Bioturbational mixing depth and carbon flux at the seafloor, *Paleoceanography*, 12, 517–526, 1997.

Valet, J.P., and L. Meynadier, Geomagnetic field intensity and reversals during the past four million years, *Nature*, 366, 234–238, 1993.

Venz, K.A., D.A. Hodell, C. Stanton and D.A. Warnke, A 1.0 Myr record of glacial North Atlantic Intermediate Water variability from ODP Site 982 in the northeast Atlantic, *Paleoceanography*, 14, 42–52, 1999.

Weeks, R., C. Laj, L. Endignoux, M. Fuller, A. Roberts, R. Manganne, E. Blanchard and W. Goree, Improvements in long-core measurement techniques: applications in palaeomagnetism and palaeoceanography. *Geophys. J. Int*. 114, 651–662, 1993.

J.E.T. Channell, Department of Geological Sciences, PO Box 112120, University of Florida, Gainesville, Florida 32611-2120

Y. Guyodo, Laboratoire des Sciences du Climat et de l'Environnement, Avenue de la Terrasse, 91198 Gif-sur-Yvette, France.